

# Tunable band-gap and isotropic light absorption from bismuth-containing GaAs core-shell and multi-shell nanowires

Muhammad Usman\*

*School of Computing and Information Systems,*

*Melbourne School of Engineering, The University of Melbourne,*

*Parkville, 3010, Victoria, Australia. and*

*School of Physics, The University of Melbourne, Parkville, 3010, Victoria, Australia.*

## Supplementary Information Document

### Analysis of strain dependent band-edge energies for GaBi<sub>x</sub>As<sub>1-x</sub>/GaAs nanowires

The band-gap energy or wavelength is investigated for GaBi<sub>x</sub>As<sub>1-x</sub>/GaAs core-shell nanowires in Figure 1 of the main text. Figure 1 (d) shows the band-gap variation as a function of the nanowire diameters for various Bi fractions. We notice that the band gap energy reduces as the diameter of the nanowire is increased at a fixed Bi composition. It is also observed that the change in the band-gap energy is slightly rapid at large nanowire diameters (variation from 35 nm to 40 nm) when compared to smaller diameters (from 25 nm to 30 nm). Since the band-gap energy is the difference between the lowest conduction band energy and the highest valence band energy, we plot the conduction and valence band energies as a function of nanowire diameter in Figure S1 (c) and (d). The changes in the band-edge energies are a result of a complex interplay between a number of effects such as quantum confinement, internal hydrostatic and biaxial strain components, random placement of Bi atoms which leads to different formation of Bi pairs and clusters (alloy disorder) and the band-gap shift due to the band anti-crossing (BAC) interaction effect [1]. Here in this section, we focus on the effect of internal strain on the band edge energies which play important role in the observed energy shifts.

The impact of internal strain on the band- edge energies is well studied in the literature in the context of deformation theory [2]. Although this simple model cannot quantitatively match the computed band edge energies due to lack of incorporation of effects from the alloy disorder and quantum confinement, it provides a qualitative understanding of band-edge energy variations on the nanowire diameters. Due to the lattice mismatch between the GaAs and GaBi<sub>x</sub>As<sub>1-x</sub> materials, both materials are under hydrostatic

---

\* [musman@unimelb.edu.au](mailto:musman@unimelb.edu.au)

and biaxial strain. We compute the strain parameters by atomistic Valence Force Field relaxation [3], which has been very accurate and widely used method for the III-V materials and nanostructures. Figure S3 (a) and (b) plot the average values of the hydrostatic and biaxial strain components at the center of the nanowire shell region at 3% and 15% Bi fractions. As the nanowire diameter is increased, both the hydrostatic and biaxial strain magnitudes decrease, which is consistent for small and large Bi fractions. However, we note that the decrease in the biaxial strain is nearly linear, whereas the relaxation of the hydrostatic strain becomes nonlinear at large nanowire diameters, exhibiting a slightly rapid relaxation when the diameter increases from 35 nm to 40 nm. This strain character can be directly related to the observed change in the band-gap energies plotted in Figure 1 (d).

The change in the strain components can be translated to the changes in the band gap energies based on the simple deformation theory:

$$\epsilon_{\text{H}} = \epsilon_{xx} + \epsilon_{yy} + \epsilon_{zz} \quad (1)$$

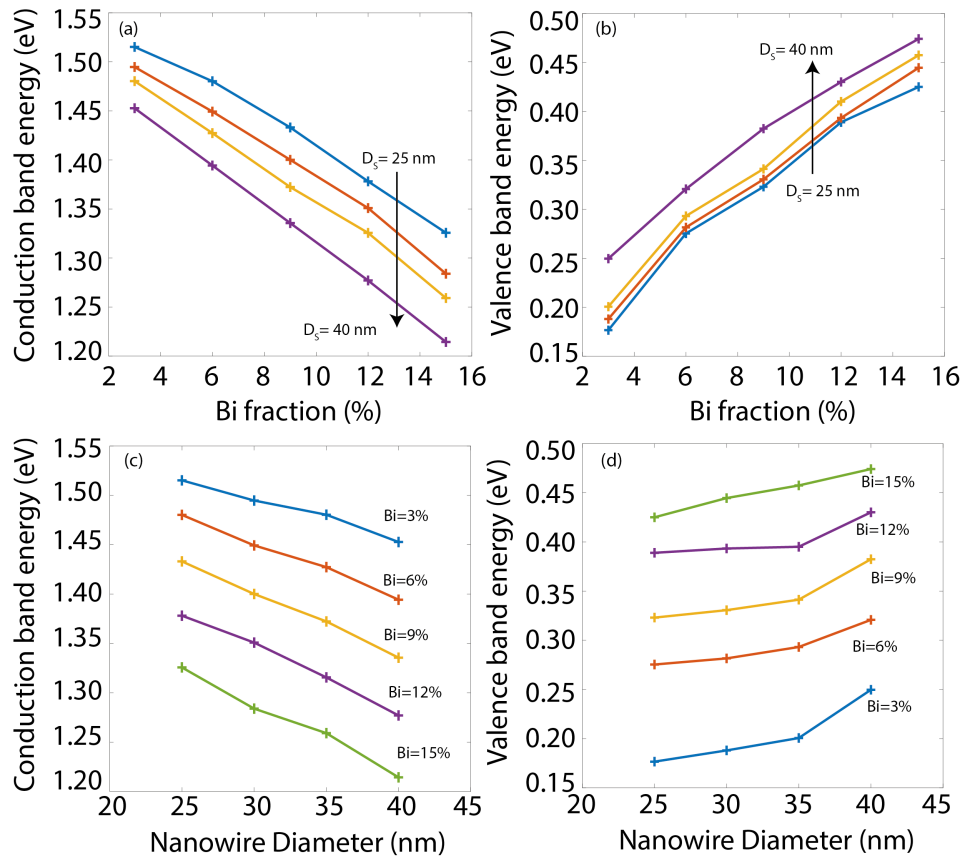
$$\epsilon_{\text{B}} = \epsilon_{xx} + \epsilon_{yy} - 2\epsilon_{zz} \quad (2)$$

$$\delta E_c = a_c \epsilon_{\text{H}} \quad (3)$$

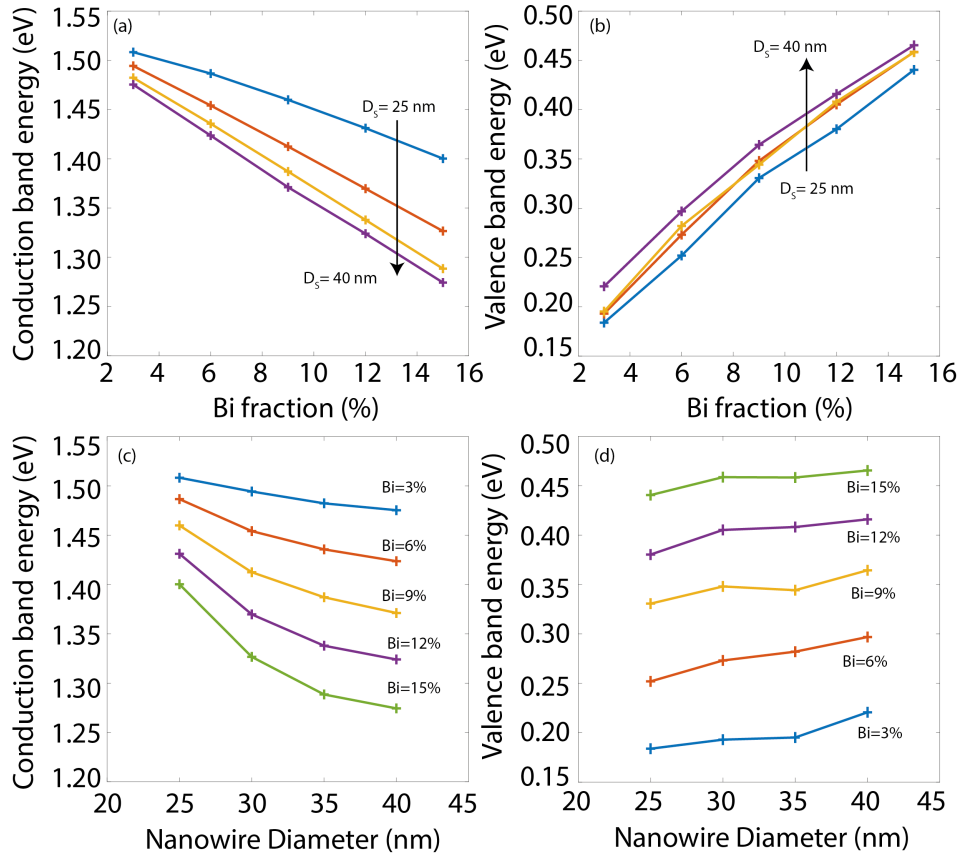
$$\delta E_v = a_v \epsilon_{\text{H}} + \frac{b_v \epsilon_{\text{B}}}{2} \quad (4)$$

$$(5)$$

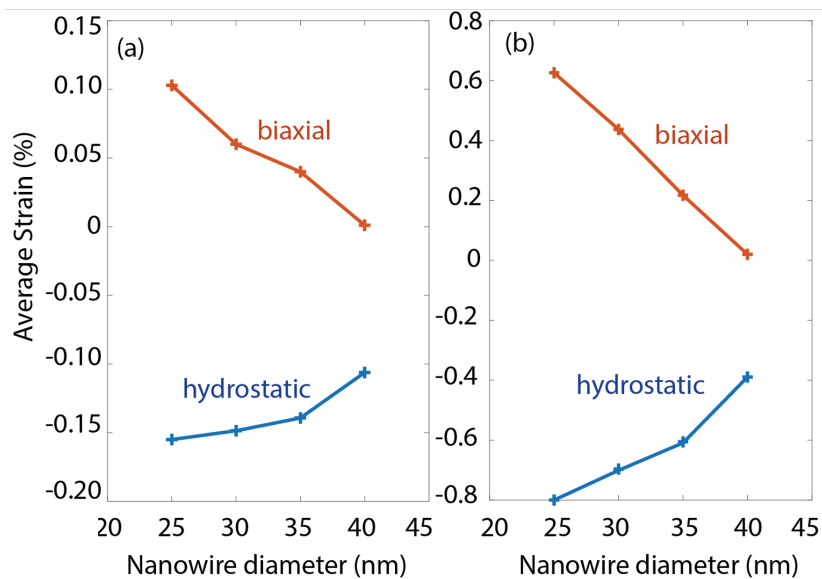
Here, the hydrostatic and the biaxial deformation potential values for the GaBiAs material are used based on the literature [4]. Based on the equations above, we compute and plot the band edge energy shifts due to the internal strain in Figure S4. These plots reveal that the overall shifts in the band edge energies due to strain roughly follow the trend computed from our full atomistic tight-binding model



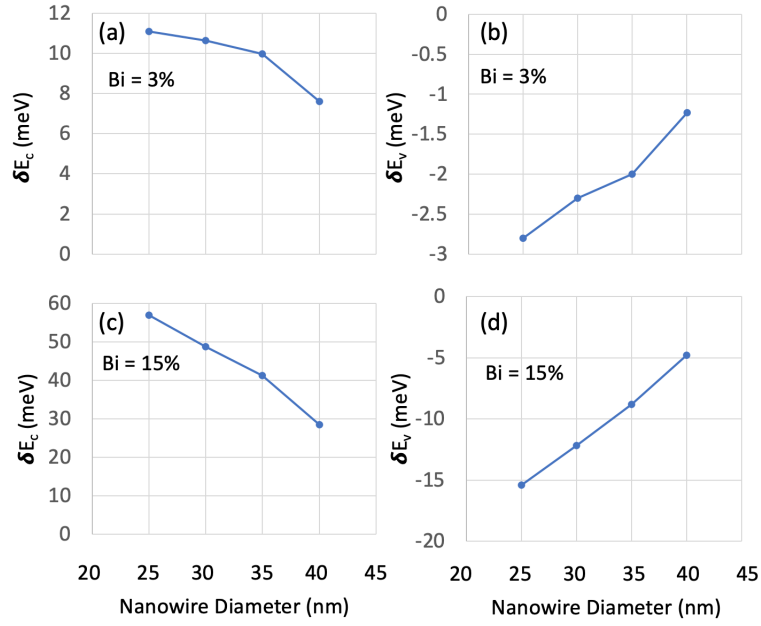
**Supplementary Fig. S1.** (a, b) The plots of the lowest conduction band and the highest valence band energy levels are shown as a function of the Bi fraction in the GaBi<sub>x</sub>As<sub>1-x</sub>/GaAs nanowires. The direction of the arrow indicates increasing diameter of the nanowire from 25 nm to 40 nm. (c, d) The plots of the lowest conduction band and the highest valence band energy levels are shown as a function of the nanowire diameter for various Bi fractions investigated in this work.



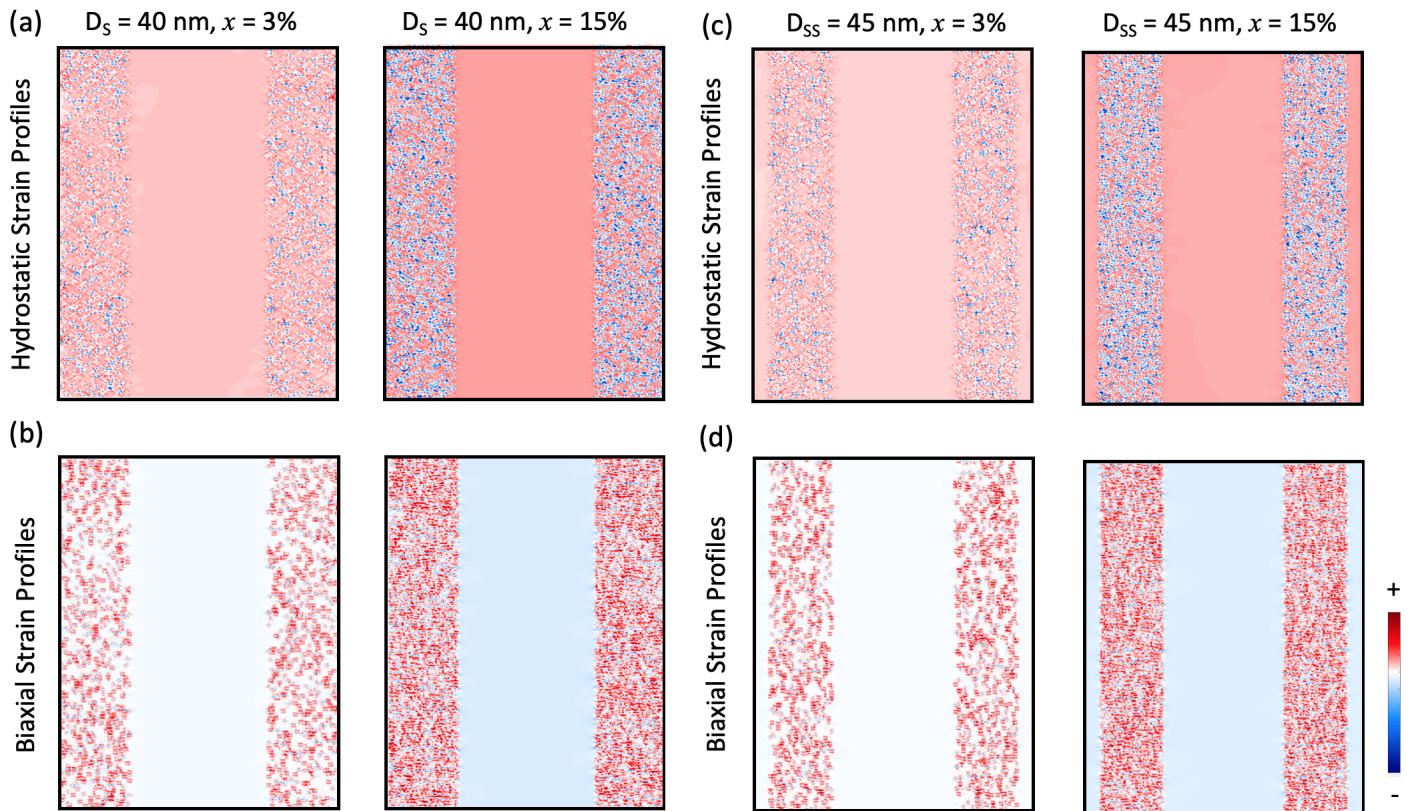
**Supplementary Fig. S2.** (a, b) The plots of the lowest conduction band and the highest valence band energy levels are shown as a function of the Bi fraction in the GaAs/GaBi<sub>x</sub>As<sub>1-x</sub>/GaAs nanowires. The direction of the arrow indicates increasing diameter of the nanowire from 25 nm to 40 nm. (c, d) The plots of the lowest conduction band and the highest valence band energy levels are shown as a function of the nanowire diameter for various Bi fractions investigated in this work.



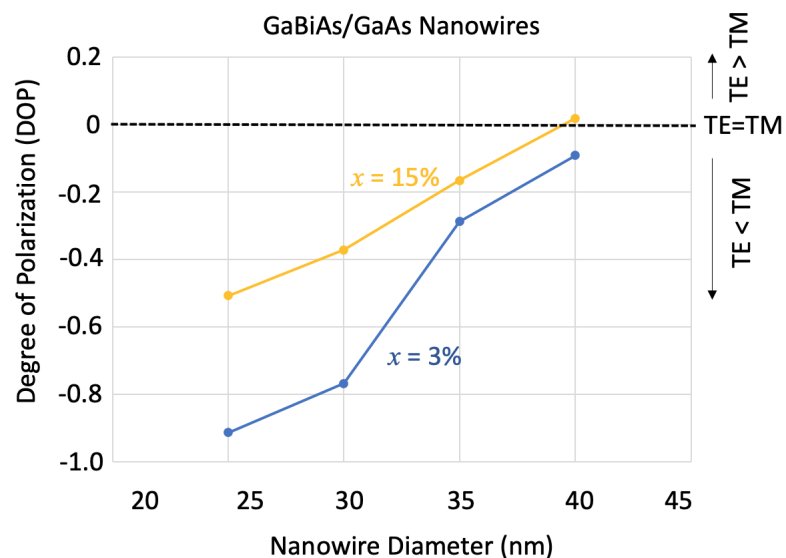
**Supplementary Fig. S3.** (a, b) The plots of average hydrostatic ( $\epsilon_H$ ) and biaxial ( $\epsilon_B$ ) strains ( $\epsilon_{xx}$ ) are shown as a function of the diameter for the GaBi<sub>x</sub>As<sub>1-x</sub>/GaAs nanowires with  $x=3\%$ , and  $15\%$ .



**Supplementary Fig. S4.** (a, b) The plots of change in the lowest conduction band edge ( $\delta E_c$ ) and the highest valence band edge  $\delta E_v$  are shown for the GaBi<sub>x</sub>As<sub>1-x</sub>/GaAs nanowire as a function of the nanowire diameter for Bi fraction of 3%. The changes in the energies are computed based on deformation potential theory. (c, d) Same as (a,b) but for Bi fraction of 15% in the nanowire shell region.



**Supplementary Fig. S5.** The strain plots are shown based on the 2D cuts through the center of the nanowire regions. The plots in the first row are for the hydrostatic component and in the second row are for the biaxial strain component. The plots in each column correspond to a selected nanowire geometry: first column is  $\text{GaBi}_x\text{As}_{1-x}/\text{GaAs}$  nanowire with diameter 40 nm and Bi fraction 3%, the second column is  $\text{GaBi}_x\text{As}_{1-x}/\text{GaAs}$  nanowire with diameter 40 nm and Bi fraction 15%, the third column is  $\text{GaAs}/\text{GaBi}_x\text{As}_{1-x}/\text{GaAs}$  nanowire with diameter 45 nm and Bi fraction 3%, and the fourth column is  $\text{GaAs}/\text{GaBi}_x\text{As}_{1-x}/\text{GaAs}$  nanowire with diameter 45 nm and Bi fraction 3%.



**Supplementary Fig. S6.** The plots of the computed degree of polarisation (DOP) are shown for  $\text{GaBi}_x\text{As}_{1-x}/\text{GaAs}$  nanowires as a function of the nanowire diameter for Bi fractions of 3% and 15%.

- 
- [1] M. Usman, C. A. Broderick, A. Lindsay, and E. P. O'Reilly, *Phys. Rev. B* **84**, 245202 (2011).
- [2] M. Usman, H. Ryu, I. Woo, D. Ebert, and G. Klimeck, *IEEE Trans. Nanotech.* **8**, 330 (2009).
- [3] P. N. Keating, *Phys. Rev.* **145**, 637 (1966).
- [4] Z. Batool, K. Hild, T. J. C. Hosea, X. Lu, T. Tiedje, and S. J. Sweeney, *J. Appl. Phys.* **111**, 113108 (2012).